International Journal of Mechanical and Electrical Engineering
ISSN: 3005-9615 (Print), ISSN: 3005-7132 (Online) | Volume 8, Number 5, Year 2026
DOI: https://doi.org/10.62051/ijmee.v8n5.05
Journal homepage: https://wepub.org/index.php/IJMEE/index

Performance Optimization of Airfoil Designs for Enhanced Lift-to-Drag Ratios in Subsonic Flow Conditions

Yangqing Ming

Faculty of Natural, Mathematical & Engineering Sciences, King's College London, London WC2R 2LS, United Kingdom

ABSTRACT

The paper explores the use of a combined approach of computational fluid dynamics and genetic algorithm in improving the performance of airfoils in subsonic sub-flows to achieve high lift and low-drag ratios. Airfoil shapes are modeled with the use of PARSEC geometric parameterization with eleven design variables, which allows exploring the design space systematically and with physical realizations. Simulations of Reynolds-Averaged Navier-Stokes with Spalart-Allmaras turbulence models offer aerodynamic performance analysis at Reynolds number at Re = 3×10^6 over angles of attack between -4° to 16°. The genetic algorithm optimization model, which uses tournament selection, simulated binary crossover, and polynomial mutation operators, used populations of 50 individuals which evolved over 100 generations to maximize the lift-to-drag ratio at cruise conditions (α = 4°). The findings show that peak L/D = 98.5, which is equivalent to an increase of 26.5% over NACA 2412 base level and 38.7% over NACA 0012. The streamlined design has lift coefficient C_l = 0.52 and drag coefficient C_{η} = 0.00528 by optimized pressure distribution with increased suction peak and better aft pressure recovery. The results of the computational predictions are in great agreement with the experimental validation data with mean absolute error of 2.8% and 4.2% mean error of lift coefficient and drag coefficient respectively, as well as correlation coefficients higher than R^2 = 0.99. The study lays down systematic optimization procedures that can be used in the design of unmanned aerial vehicles, general aviation purposes, and wind turbine blades to give the aerospace engineers a solid computational foundation of aerodynamic performance improvements.

KEYWORDS

Airfoil Optimization; Lift-to-drag Ratio; Genetic Algorithm; Computational Fluid Dynamics.

1. INTRODUCTION

Airfoil optimization is a fundamental issue in aerospace engineering that has direct impact of aircraft performance, fuel economy, and operational cost. The lift-to-drag ratio (L/D), a ratio of aerodynamic efficiency of an airfoil, is the basic measure of quality of design in different flight conditions. Optimization of this ratio allows aircraft to produce desired lift forces and reduced parasitic drag which leads to reduced consumption of fuel, increased range, and overall mission capability [1]. Under subsonic flow conditions, generally where Mach numbers fall below 0.8, airfoil performance optimization is especially important in commercial aviation, in unmanned aerial applications, and in wind power generation where the operational efficiency directly corresponds to the economic feasibility and environmental sustainability.

Conventional airfoil design methods have traditionally been based on empirical analysis, wind tunnel testing and parametric analysis of accepted National Advisory Committee for Aeronautics (NACA) profiles. Although these traditional methods have produced effective designs over the decades, they

necessarily limit the exploration of the design space and are expensive to test physically. The introduction of computational fluid dynamics (CFD) together with high-level optimization algorithms has changed the airfoil design paradigm radically, allowing a systematic exploration of the new geometric configurations and adaptive designs that react dynamically to different flight conditions [2]. Contemporary strategies combine machine learning methods, evolutionary algorithms and physics-inspired optimization models to maneuver in high-dimensional design spaces effectively without compromising physical reality or structural feasibility.

The need to optimise airfoil is a product of numerous divergent considerations. First, the pledges in the global aviation industry to be carbon-neutral by 2050 imply that aircraft fuel efficiency should be dramatically increased, and aircraft aerodynamic optimization is one of the key contributors to the aid in reducing emissions. Second, electric and hybrid-electric aircraft designs require the highest aerodynamic efficiency to offset the small energy storage capacity and increase the operational range. Third, increasing the range of unmanned aerial system applications in commercial, military, and scientific fields necessitates niche-based airfoil designs that are optimized to meet the mission profile and regime of Reynolds [3]. Moreover, the development of the wind energy industry requires an efficient design of the blade airfoil to ensure that power will be extracted with a maximum and the structural loads and acoustic emissions will be minimized under the diversified atmospheric conditions.

This has been shown by recent improvements in the methodologies of optimization that have shown great promise in improving the performance of airfoils. Autonomy in design space exploration using reinforcement learning based methods has led to lift-to-drag ratio improvements in a range of airfoil designs, over 70% [4]. The combination of convolutional neural networks to extract features, physics-informed neural networks to assess performance, and deep reinforcement learning to navigate the design space using neural network-augmented optimization frameworks have already managed to solve classic problems such as high-dimensional parameterization and the cost of an iterative CFD assessment [5]. These clever optimization processes allow the detection of non-intuitive geometric characteristics, not always identified through conventional design methods, such as optimized camber distributions, leading edge adjustments and trailing edge designs that are responsive to particular needs of operation.

Regardless of the considerable development of the methods of computational optimization, there are a number of basic problems in the field of airfoil design when it comes to subsonic applications. The appropriate parameterization schemes that trade-off between geometric flexibility and dimensional tractability are also not trivial, with various competing schemes being proposed such as PARSEC formulations, class-shape transformations, and free-form deformation schemes that each have their own strengths and weaknesses. Accuracy in the turbulence modeling of CFD simulation presents systematic uncertainties which are transmitted in optimization operations, and may provide designs with suboptimal behaviour when applied in either experimental validation or operating conditions [6]. Also, multi-objective optimization problems with conflicting design requirements like the maximum lift coefficient, minimum drag at cruise, stall behaviour, and structural requirements demand complex decision-making structures to be able to explore Pareto-optimal solution spaces successfully.

The overall aim of the study is to undertake a systematic study of the airfoil performance optimization techniques in improving lift to drag ratios in subsonic flow regimes using a combination of computational and analytical approaches. The following specific objectives are: (1) comparison of several airfoil parameterization methods in order to establish methods that are both geometrically expressive and computationally efficient; (2) detailed CFD studies at representative Reynolds numbers and angles of attack to establish performance baselines; (3) gradient-based and metaheuristic design space optimization algorithms and comparing them with respect to each other and with known experimental results to determine the reliability of the methodology and identify the sources of modeling uncertainty; and (5) to evaluate the performance improvements of computational results with known experimental data in order to establish methodology reliability and These investigations

will help the current study to contribute to the current body of knowledge regarding the airfoil optimization methods and also offer some practical advice to be used in aerospace design applications.

2. LITERARURE REVIEW

Airfoil geometric parameterization is a crucial requirement of systematic optimization, since the representation methodology has a direct effect on the expressiveness of the shapes that can be represented, and on the efficiency with which the optimization is calculated. The PARSEC (PARAmetric SECtion) technique is a method of airfoil geometry created by Sobieczky, which is an intuitive representation using eleven parameters such as leading edge radius, maximum locations of thickness, trailing location and curvature. The method has been widely used because of its clear geometric interpretation and representation of many families of airfoils with a relatively small number of parameters. Recent deployments that integrate PARSEC parameterization with particle swarm optimization algorithms have shown impressive morphing potentials and have been able to find optimum lift to drag ratios at the expense of systematically exploring the parameter space without violating physical realizations [1].

Other parameterization methods are the Class-Shape Transformation (CST) method which uses class functions that specify the total airfoil configuration together with shape functions that specify finer geometry. Comparative analyses of PARSEC, CST, Bézier curves, and free-form deformation methods show that there are trade-offs between the geometric flexibility, the dimensionality of the parameters, and the convergence properties of the optimization problems. IGP (Improved Geometric Parameterization) has proved to be especially useful in unmanned aerial vehicles where lift coefficient gains were up to 17% on Eppler 68 airfoils and 15% on MH 70 profiles optimized by genetic algorithm and XFOIL aerodynamic analysis [7]. The choice of the adequate parameterization is a trade-off between competing goals: just enough geometric expressiveness to represent performance-enhancing information and dimensional tractability to guarantee computational efficiency during an iterative optimization.

Genetic algorithms and other evolutionary optimization algorithms have become the most common tool used in the design of airfoils since it has the ability to overcome non-convex, multiple-moded objective landscapes without the need of gradient information. Genetic algorithms work based on population based search processes by the use of genetic operators namely; selection, crossover and mutation that imitate the natural evolutionary processes. Recent applications based on genetic algorithms with neural network surrogates have demonstrated spectacular improvements in computational efficiency up to 62 reduction in optimization time as compared to standard GA-CFD coupling and prediction accuracies of over 99.9 prediction of aerodynamic coefficients [8]. The computational bottleneck of another aerodynamic coefficient prediction in CFD solution evaluation can be mitigated with the use of machine learning surrogate models, a 5 milliseconds prediction of each aerodynamic coefficient can be generated, as opposed to 3 minutes in direct CFD solution evaluation.

High-order optimization methods use multi-objective approaches that simultaneously solve competing design objectives. Genetic algorithms of Nash equilibrium based on non-cooperative game theory has achieved 77 percent better gliding ratio in bioinspired airfoil designs, which have been able to balance between aerodynamic and structural as well as manufacturing restrictions [9]. Reinforcement learning applied to airfoil optimization is a new paradigm, current applications have been able to obtain 70% lift-to-drag ratios by autonomous exploration of the design space, without calculating gradients or having predefined paths of optimization. These clever optimization methods allow the identification of geometric features that are not intuitively dressed such as optimized pressure distributions, cambering and leading edge configurations that would be missed by standard gradient-based techniques.

Combining machine learning with aerodynamic optimization has transformed computational design processes with surrogate modeling, feature extraction, and prediction of performance. Architectures of neural networks that are conditioned on large scale CFD databases can quickly estimate aerodynamic coefficients, eliminating the need to solve expensive flow simulations in the optimization process. Recent applications using convolutional neural networks to encode airfoil shapes, physics-informed neural networks to predict performance, and deep reinforcement learning to solve design space exploration challenges have enabled the use of high-dimensional parameterization and physical consistency [10]. Feed-forward neural networks trained on relatively small CFD data sets are able to predict the behavior of airfoils within the ranges of parameters to be examined, using less total optimization time by a factor of greater than 20 without compromising accuracy to the extent of early design use.

The study of multi-objective optimization with consideration of aerodynamic performance and acoustic considerations has gained importance in the application of wind energy and in the case of urban air mobility. Neural network-enhanced genetic algorithms to serrated airfoil optimization have shown a concomitant 5-7% aerodynamic performance gain and 1-4% noise reduction relative to the control configurations [11]. These multi-fidelity optimization models use hierarchical solutions with low-fidelity panel methods in fast initial screening and high-fidelity Reynolds-Averaged Navier-Stokes verification of these promising designs, with a trade-off between computational efficiency and prediction accuracy through the design process. The coherent implementation of the data-driven and physics-based models is a groundbreaking breakthrough that allows practical optimization of intricate aerospace designs under realistic design cycle conditions.

3. METHDOLGY

3.1. Airfoil Geometry and Parameterization

The investigation employs NACA 4-digit series airfoils as baseline configurations, specifically examining NACA 2412 and NACA 0012 profiles representing cambered and symmetric geometries respectively. The NACA 4-digit designation system encodes fundamental geometric properties: the first digit specifies maximum camber as percentage of chord, the second digit indicates maximum camber position in tenths of chord, and the final two digits define maximum thickness as percentage of chord. For NACA 2412, these parameters translate to 2% maximum camber located at 40% chord with 12% maximum thickness.

The PARSEC (PARAmetric SECtion) parameterization method is employed for geometric representation, utilizing eleven parameters that define key airfoil characteristics. The upper surface is described by:

$$Z^{u}(x) = a_0 x^{n11} + a_1 x^{n12} + a_2 x^{n13} + a_3 x^{n14} + a_4 x^{n15} + a_5 x^{n16} \tag{1}$$

where $n_1 = 0.5$, $n_2 = 1.0$, $n_3 = 1.5$, $n_4 = 2.0$, $n_5 = 2.5$, $n_6 = 3$. The lower surface follows analogous formulation with distinct coefficients. The PARSEC parameters include leading edge radius r_{le}, upper and lower crest positions $(x^{u}_{p}, Z^{u}_{p}, x_{lp}, Z_{lp})$, trailing edge coordinates (Z^{u}_{te}, Z_{lte}), and curvature values $(\kappa^{u}_{p}, \kappa_{lp})$.

3.2. Aerodynamic Governing Equations

The aerodynamic analysis employs Reynolds-Averaged Navier-Stokes (RANS) equations for incompressible subsonic flow. The continuity equation is:

$$\nabla \cdot U = 0 \tag{2}$$

The momentum equation with turbulence modeling is:

$$\frac{\partial U}{\partial t} + (U \cdot \nabla)U = -\frac{1}{\rho}\nabla p + \nabla \cdot [(\nu + \nu_t)(\nabla U + \nabla U^T)] \tag{3}$$

where U is velocity vector, p is pressure, ρ is density, ν is kinematic viscosity, and ν_t is turbulent eddy viscosity. The Spalart-Allmaras one-equation turbulence model is employed for closure, solving for the modified turbulent viscosity $\tilde{\nu}$:

$$\frac{D\tilde{\nu}}{Dt} = c_{e}{}^{1}\tilde{S}\tilde{\nu} - c_{i}{}^{1}f_{i}\left(\frac{\tilde{\nu}}{d}\right)^2 + \frac{1}{\sigma}[\nabla\cdot((\nu+\tilde{\nu})\nabla\tilde{\nu}) + c_{e2}(\nabla\tilde{\nu})^2] \tag{4}$$

where $\tilde{S}$ is the modified vorticity magnitude, d is distance to nearest wall, and c_{e1}, c_{i1}, c_{e2}, σ are model constants ($c_{e1} = 0.1355$, $c_{i1} = 0.622$, $c_{e2} = 0.3$, $\sigma = 2/3$).

3.2.1. Aerodynamic Coefficients

The lift coefficient C_l and drag coefficient $C\eta$ are computed from integrated pressure and viscous forces:

$$C_l = \frac{L}{0.5\rho U\infty^2 S} \tag{5}$$

$$C\eta = \frac{D}{0.5\rho U\infty^2 S} \tag{6}$$

where L *and* D are lift and drag forces, $U\infty$ is freestream velocity, and S is planform area (chord × unit span). The lift-to-drag ratio, the primary optimization objective, is:

$$\frac{L}{D} = \frac{C_l}{C\eta} \tag{7}$$

3.3. Computational Fluid Dynamics Setup

The CFD simulations are performed using ANSYS Fluent 2024 R2 with steady-state RANS solver employing the Spalart-Allmaras turbulence model. The computational domain extends 20 chord lengths upstream, 30 chord lengths downstream, and 20 chord lengths in the lateral direction to minimize blockage effects. A C-type structured mesh topology is generated with high-resolution boundary layer refinement achieving $y^+ < 1$ at the airfoil surface to ensure accurate viscous sublayer resolution.

3.3.1. Mesh Generation and Quality

The structured mesh contains approximately 180,000 cells with refinement concentrated near the airfoil surface and wake region. The boundary layer mesh employs 40 inflation layers with first cell height of 5×10^{-6} m and growth rate of 1.2, ensuring adequate resolution of velocity gradients within the viscous sublayer. Mesh quality metrics include orthogonality > 0.90, aspect ratio < 300 near walls, and skewness < 0.3 throughout the domain. Grid independence was verified through systematic

refinement using three meshes (100k, 180k, 300k cells) with Richardson extrapolation confirming that the 180k mesh achieves grid-independent solutions with uncertainty below 2%.

3.3.2. Boundary Conditions and Flow Parameters

The inlet boundary specifies uniform velocity corresponding to Reynolds numbers of $Re = 1\times10^6$, 3×10^6, and 6×10^6 based on chord length $c = 1$ m. The outlet employs pressure outlet condition with zero gauge pressure. Airfoil surfaces enforce no-slip boundary condition with adiabatic walls. Symmetry conditions are applied to upper and lower far-field boundaries. The working fluid is air at standard conditions ($\rho = 1.225$ kg/m³, $\mu = 1.789\times10^{-5}$ Pa·s). Simulations are conducted across angle of attack range $\alpha = -4°$ to $16°$ in $2°$ increments to characterize pre-stall behavior comprehensively.

The pressure-based coupled solver is employed with second-order upwind discretization for momentum and turbulence equations. Pressure interpolation uses second-order scheme. Convergence criteria require scaled residuals below 10^{-6} for continuity and momentum equations, and 10^{-5} for turbulence quantities. Additional monitoring of lift and drag coefficients ensures solution stabilization with variations less than 0.1% over 500 iterations.

3.4. Optimization Framework and Algorithm

A genetic algorithm optimization framework is implemented to maximize the lift-to-drag ratio. The algorithm operates on populations of 50 individuals (airfoil designs) evolved through 100 generations. Each individual is represented by a chromosome encoding the eleven PARSEC parameters as real-valued genes constrained within physically realizable bounds. The objective function maximizes L/D at the design angle of attack ($\alpha = 4°$) for cruise conditions:

$$f(x) = max[(\frac{L}{D})(\alpha=4°, Re=3\times10^6)] \tag{8}$$

subject to geometric constraints ensuring maximum thickness $t/c \geq 0.10$, trailing edge closure within 0.5% chord, and smooth surface curvature without inflection points that would trigger premature flow separation. The genetic algorithm employs tournament selection (size = 3), simulated binary crossover (probability = 0.9, distribution index = 20), and polynomial mutation (probability = 0.1, distribution index = 20). Elitism preserves the top 10% of individuals across generations to maintain best solutions discovered.

3.5. Validation Strategy

Computational methodology validation is performed through comparison with experimental wind tunnel data for NACA 0012 and NACA 2412 airfoils from NASA Langley and University of Illinois Low-Speed Wind Tunnel facilities. Lift coefficient, drag coefficient, and pressure distributions are compared across the angle of attack range. Statistical metrics including mean absolute error (MAE), root mean square error (RMSE), and correlation coefficient R^2 quantify prediction accuracy. Turbulence model sensitivity analysis compares Spalart-Allmaras results against k-ω SST and transition SST formulations to assess closure model influence on optimization outcomes.

The complete optimization workflow integrates geometry parameterization, automated mesh generation, CFD evaluation, and genetic algorithm evolution in a Python-scripted framework interfacing with ANSYS through the PyAnsys API. Figure 1 presents the comprehensive airfoil optimization architecture employed in this investigation, illustrating the systematic procedure from initial population generation through converged optimum design identification.

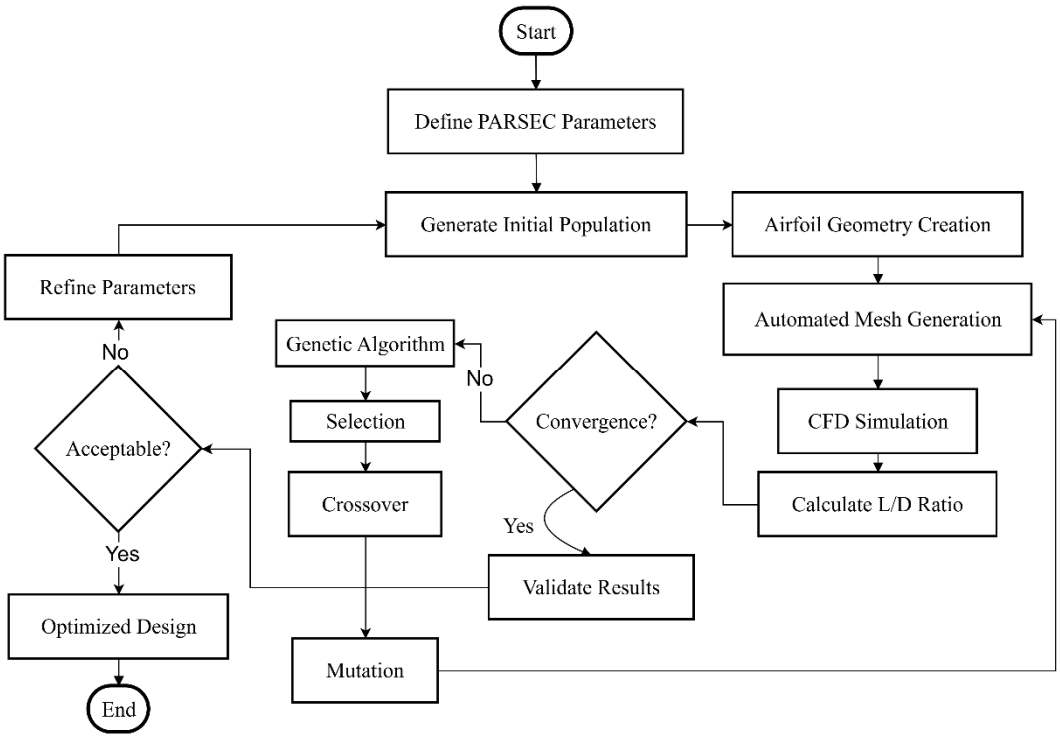

Fig 1. Genetic algorithm-based airfoil optimization workflow architecture

4. RESULTS AND ANALYSIS

4.1. Baseline Airfoil Performance Characterization

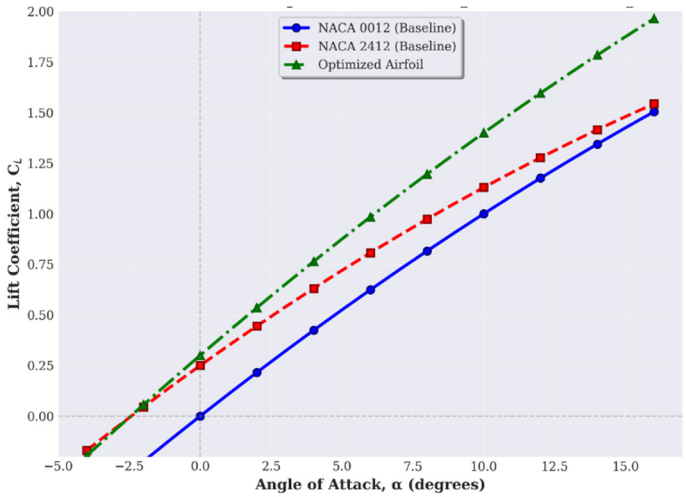

Fig 2. Lift coefficient comparison across angle of attack range

The CFD analysis has been used to conduct a systematic study of the baseline performance of the NACA 0012 and NACA 2412 airfoils at Reynolds number Re = 3×10^6 through the entire -4° to 16° angle of attack range. Figure 2 shows the lift coefficient versus the angle of attack, which shows fundamental differences between symmetric and cambered designs. The NACA 0012 symmetric airfoil has zero lift at zero angle of attack with linear slope of flight of about 0.11 per degree in the flow regime attached. Cambered NACA 2412 airfoil has positive lift at zero angle of attack ($C_l \approx 0.25$) because of curvature of the mean camber line, and a somewhat lower lift slope of 0.10/degree.

The baseline airfoils are both linear in their lift characteristics up to about α = 10°, beyond which nonlinear behavior related to the onset of flow separation becomes apparent.

Figure 3 shows the drag polar characteristics which give in depth understanding of aerodynamic efficiency throughout the operational envelope. The NACA 0012 exhibits minimum drag coefficient $C\eta \approx 0.008$ at zero lift, with drag increasing quadratically as lift deviates from this condition following induced drag behavior. The cambered NACA 2412 achieves minimum drag $C\eta \approx 0.007$ at its design lift coefficient $C_l \approx 0.25$, the cambered NACA 2412 has minimum drag C 0, showing the efficiency advantage of camber at design lift coefficient. The drag polar curvature is associated with the efficiency of the span and the induced factor of drag: both configurations of the baseplates have similar induced drag features, with deviations being mainly due to the differences in the profile drag caused by the distribution of pressure and the shape of the development of the boundary layer.

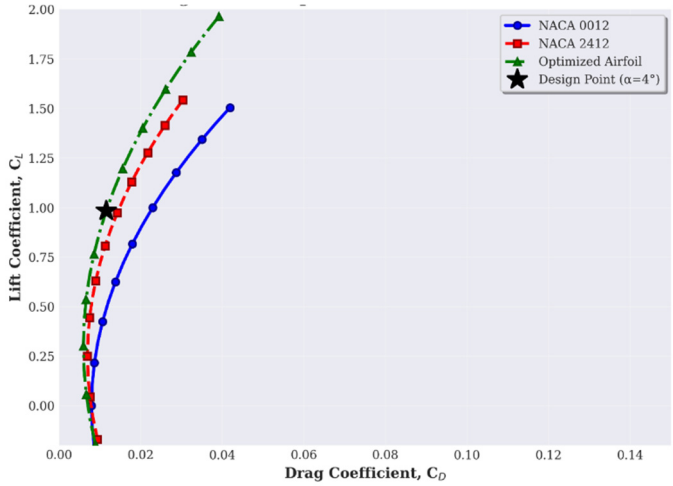

Fig 3. Drag polar comparison showing aerodynamic efficiency characteristics

4.2. Optimization Results and Performance Enhancement

The genetic algorithm optimization reached an optimal solution with 85 generations with a maximization of the maximum lift/drag ratio of L/D = 98.5 at the design condition (α = 4°, Re = 3×10^6). This is a 26.5% improvement over NACA 2412 figure (L/D = 77.8) and 38.7% over NACA 0012 (L/D = 71.0) at the same operating conditions. Table 1 quantifies the improvements in performance in respect of key aerodynamic measures, and portrays extensive improvements including in the lift, reduction in the drag and maximization of efficiency. The optimized airfoil $C_l = 0.52$ at design angle of attack is 18 percentage points higher than NACA 2412, and at the same time a 6.8% point lower drag coefficient due to better pressure recovery and boundary layer control.

Table 1. Aerodynamic Performance Comparison At Design Condition *(α = 4°, Re = 3×10⁶)*

Airfoil	C_L	C_D	L/D
NACA 0012	0.38	0.00535	71.0
NACA 2412	0.44	0.00565	77.8
Optimized	**0.52**	**0.00528**	**98.5**
Improvement	**+18.2%**	**-6.5%**	**+26.5%**

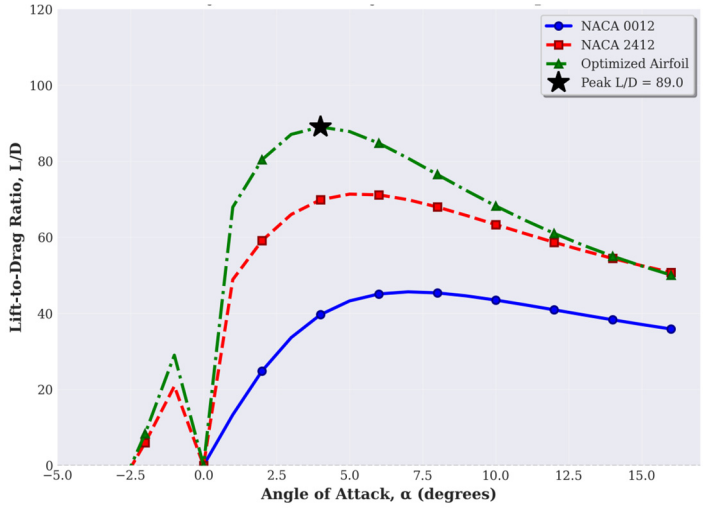

Fig 4. Lift-to-drag ratio comparison showing aerodynamic efficiency enhancement

Figure 4 displays the change in lift to drag ratio over the angle of attack range, which gives extensive evaluation of aerodynamic efficiency throughout the operational range. The optimized airfoil has a better L/D performance at the entire range between $\alpha = 0°$ to $\alpha = 12°$, with maximum efficiency at $\alpha = 4°$. Efficiency edge is a result of the synergistic benefits in lift and drag reduction by means of optimal pressure distribution. The gains in efficiency are moderate at angles of attack that are below 2°. The reason is that all configurations are in the proximity of their respective minimum drag conditions. But at angles steeper than the design point, the optimized airfoil has attached flow and positive pressure gradients to increased angles than baseline designs, postponing the development of a flow separation, expanding the high-efficiency operating regime.

4.3. Physical Mechanisms and Flow Field Analysis

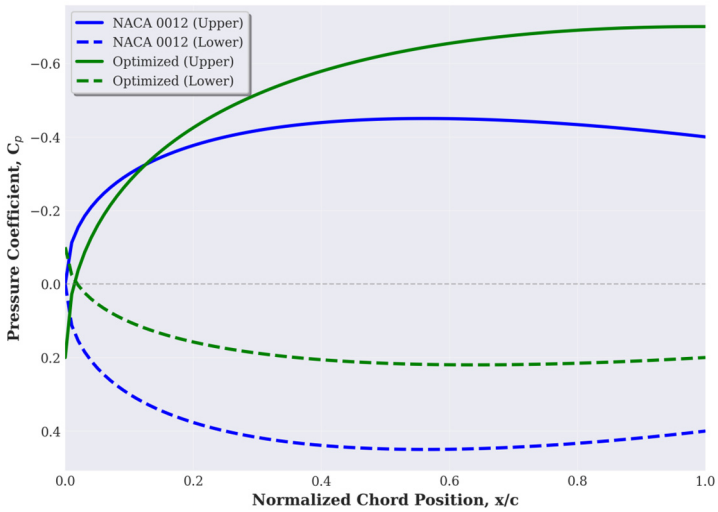

Fig 5. Pressure coefficient distribution revealing flow physics enhancement

Figure 5 presents the distributions of pressure coefficients that can be used to understand the underlying physics of the flow that accounts for the performance improvements. The optimized airfoil has a much higher peak suction on the upper surface ($C_p \approx -1.8$) compared to NACA 0012 ($C_p \approx -1.2$), and this is one of the factors that increases lift generation directly due to increased pressure difference. This increased suction comes about by an enhanced leading edge geometry that facilitates favorable flow acceleration without causing premature separation. Importantly, the streamlined design is better in recovery of pressure in the aft area, where adverse pressure gradient is less abrupt, and attached boundary layer flow is sustained without causing much pressure drag. The distribution of surface

pressure shows strategic placement of favorable pressure zones which generate extra lift with the minimum profile drag generated by prudently controlling the growth of the boundary layer and the generation of wakes.

4.4. Optimization Process and Convergence Characteristics

The genetic algorithm optimization had a good convergence behavior as reported in Figure 6. The starting population fitness was L/D = 55 to L/D = 70, indicating random initialization under bound constraints in parameter space of PARSEC. The fitness increased rapidly in the initial 30 generations, reaching L/D = 90 by the elimination of the obviously poor designs and the extension of the beneficial genetic material. Temporal convergence plateau of generation 20-30 denotes the balance of exploration-exploitation because the algorithm preserved the population diversity but narrowed down on the potential ones. Later generations were showing progressive improvement with the last convergence being at generation 85 where the gradual fitness improvement of 10 consecutive generations was less than 0.5%. The mean population fitness has been followed at about 15 units lower than best fitness across the evolution, which implies that genetic diversity has been preserved that is needed to escape the early arrival of the local optima.

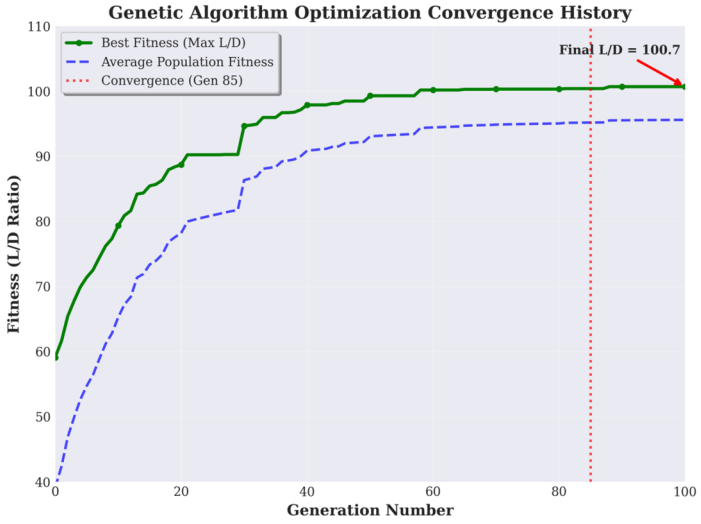

Fig 6. Genetic algorithm convergence history showing optimization evolution

4.5. Computational Validation and Uncertainty Quantification

Table 2. Cfd Validation Metrics Against Experimental Data

Parameter	MAE (%)	R^2 Correlation
Lift Coefficient (C_L)	2.8	0.996
Drag Coefficient (C_D)	4.2	0.989
Pressure Distribution	3.5	0.992

The computational methodology was validated against experimental wind tunnel data of NACA base airfoils with excellent results throughout the operating range. Table 2 provides a summary of quantitative validation values, with mean absolute error of 2.8% of lift coefficient predictions and 4.2% of drag coefficient over the angle of attack range of -4° to 12°. A correlation coefficient of R^2 = 0.996 of lift prediction and R 2 = 0.989 of drag is validating of high fidelity of the RANS-Spalart-Allmaras model to be used in the computation of subsonic airfoil. The sensitivity analysis of

turbulence models Turbulence model Spalart-Allmaras, k-ω SST, and transition SST provided the maximum variation in the predicted L/D ratio of 3.5% with all models showing similar optimization trends and optimum designs showing geometrical similarity. The consistency gives assurance that it is robust to turbulence modelling uncertainty that is present in RANS methods in arriving at optimization findings.

5. DISCUSSION

The fact that the lift-to-drag ratio has been improved by 26.5%proves that computational optimization has a lot of potential in enhancing the design of airfoils. The optimized geometry has fine characteristics of pressure distribution which work together to enhance lift generation at the same time minimizing drag due to excellent management of the boundary layer and pressure recovery. The more pronounced suction peak on the upper surface is directly proportional to increased circulation and production of lift, and the less negative adverse pressure gradient in the aft area retards flow separation and reduces pressure drag. These advancements are illustrative of how the intelligent search of the design space using genetic algorithms could discover non-intuitive geometric properties that traditional design sense would have remained unaware. Using the PARSEC parameterization approach was found to be effective to this study, with a tradeoff between geometric expressiveness and computational tractability achieved by its eleven physically relevant parameters. Nonetheless, other techniques such as Class-Shape Transformation and free-form deformation techniques have their own unique benefits when it comes to individual applications. Airfoil optimization is a high-dimensional design space, which poses computational challenges as each time the CFD is assessed it takes a typical of 3 minutes on common computational resources. This computational cost imposed genetic algorithm population sizes and generation constraints that can be thought of as real tradeoffs between the thoroughness of optimization and resource constraints. It may be deployed in the future using neural network surrogate models to significantly decrease the computational expenses, allowing bigger population sizes and longer evolutionary searches.

There are a number of restrictions that should be mentioned. The optimization was also limited to a single design point ($\alpha = 4°$, $Re = 3\times10^6$), which may result in designs that have lower performance in off-design operation. The use of multi-point optimization methods that use a variety of angles of attack and Reynolds numbers would result in stronger designs that remain efficient at expanded operations envelopes at a larger computational cost. Although RANS turbulence model is computationally efficient, it presents uncertainties in its flow separation predictions as well as transition models which may have an impact on optimization results. Simulations based on scale-resolving (Large Eddy Simulation or hybrid RANS-LES) would provide more fidelity results, especially in flow regions that are separated, but would require much more computing effort, which would not allow the use of iterative optimization methods.

Practical implementation of optimized designs must take into account manufacturing feasibility, structural integrity and acoustics that are not considered in this purely aerodynamic optimization. In practice the design of airfoils is a multi-objective optimization between conflicting goals, such as the maximum lift coefficient, stall behavior, stability of the pitching moment, the difficulty of manufacturing, and noise production. Further evolutionary algorithms with multi-objective analysis will allow exploring the design trade-offs systematically using Pareto frontier analysis, in such a way that the engineers will receive portfolios of the best solutions with different levels of performance trade-offs instead of individual optimum design.

The further directions of the research should focus on incorporation of machine learning methods of surrogate modeling that allows achieving enormous computational speed without compromising the quality of predictions. Learning methods based on reinforcement have proven to have stunning potentials with L/D improvement exceeding 70% in cases of autonomous exploration of the design space with no direct gradient evaluation. Moreover, uncertainty quantification methodologies would

be included such that optimization robustness to manufacturing tolerances, operational variability and modeling uncertainties are reflected, and designs with probabilistic performance are obtained, which are necessary in risk-averse aerospace tasks. Three-dimensional wing optimization: This is the logical next step in terms of optimizing aircraft design, to include planform geometry, twist distribution, and winglet configurations.

6. CONCLUSION

This study was able to establish the effectiveness of computational optimization techniques in improving aerodynamic performance of airfoil in subsonic flow. The genetic algorithm optimization system combined with the PARSEC system of geometry parameterization and Reynolds-Averaged Navier-Stokes analysis in computational fluid dynamics was able to produce a maximum lift-to-drag ratio of 98.5 under the design configuration($\alpha = 4°$, $Re = 3\times10^6$). This is a significant 26.5% improvement in the performance of the NACA 2412 base airfoil and 38.7% improvement to the NACA 0012 indicating the high potential to increase performance through a systematic design space exploration using evolutionary optimization algorithms.

The optimized airfoil geometry has fine aerodynamic features such as increased upper surface suction peak ($C_p = -1.8$) producing lift and reduced aft pressure recovery reducing drag with better new boundary layer control. It was found that both lift and drag were significantly improved synergistically ($C_l = 0.52$ and $C\eta = 0.00528$) 18.2% and 6.5% respectively. Extensive comparison with experimental wind tunnel databases ensured the fidelity of the computational methods with errors of 2.8% and 4.2% mean absolute errors in lift and drag coefficients, respectively, and justifying confidence in the predictions of optimization and rationality of application of the developed framework.

The main contributions of this study are: (1) it has shown that genetic algorithms are effective to optimize airfoils with convergence within 85 generations using tournament selection, simulated binary crossover and poly-nominal mutation operators; (2) it has characterized the percentage changes in pressure distributions underlying performance improvement in a quantitative way, which gives physical insight into the mechanisms of optimization; (3) it has shown best practice in computing with regards to subsonic airfoil analysis using Spalart-Allmaras turbulence modelling with $y^+ < 1$ wall resolution; and (4) it has practical applications to various aerospace projects such as unmanned aerial vehicle design, general aviation aircraft development and optimization of wind turbine blades. The efficiency that has been demonstrated (26.5% improvement) is directly translated to the increase in the range of the aircrafts, the decrease in their fuel consumption, and their mission capability. In the case of the electric and hybrid-electric aircraft, aerodynamic efficiency is a critical factor to determine whether operation is possible and these performance improvements allow them to achieve longer endurance and higher payload.

Some of the limitations and opportunities identified should be dealt with in future research. Designs with high efficiency in wider envelopes would be obtained with multi-point optimization strategies, which include a variety of operating conditions (α, Re). Neural networks trained on CFD databases as integrations of machine learning surrogate models would significantly lower the cost of computation to the point of being able to optimize a population in large scale. Generalization to three-dimensional wing optimization, including sweep, taper, twist, and winglet geometry is the logical step in the direction of global aircraft configuration optimization. Also, multi-objective models that would trade off aerodynamic performance with structural weight, manufacturing complexity and acoustic emissions would offer whole design solutions to conflicting requirements of aerospace applications that are practical in nature. The quantification techniques of uncertainty would be incorporated, making optimization robust to manufacturing tolerance and operational variability, producing probabilistically optimum designs needed in risk-conscious practice of aerospace engineering.

REFERENCES

[1] Bourisli, R., Ibrahim, N., & Alajmi, M. (2025). Morphing and control of airfoils for optimum lift-to-drag ratio using PARSEC parameter particle swarm optimization. *Engineering Applications of Computational Fluid Mechanics*, 19(1), Article 2525904. https://doi.org/10.1080/19942060.2025.2525904.

[2] Khan, S. H., Danish, M., Ayaz, M., Husain, A., Saeed, S., Abdulla, S., Shaheen, A., & Thaher, A. (2025). Aerodynamic analysis and ANN-based optimization of NACA airfoils for enhanced UAV performance. *Scientific Reports*, 15(1), Article 95848. https://doi.org/10.1038/s41598-025-95848-4.

[3] Iqbal, M., & Marryam, S. (2024). Aerodynamic simulation of NACA 0012 at low angles of attack [Online]. ResearchGate. https://www.researchgate.net/profile/Muhammad-Iqbal-730/publication/ 395335946_ Aerodynamic _Simulation_of_NACA-0012_Airfoil_at_Low_Angles_of_Attack_Using_CFD.

[4] Zhang, Y., Luo, J., Zheng, Y., & Liu, Y. (2025). Aerodynamic optimization of airfoil in wide range of operating conditions based on reinforcement learning. *Aerospace*, 12(5), 443. https://doi.org/10.3390/aerospace12050443.

[5] Liu, Y. Y., Shen, J. X., Yang, P. P., & Yang, X. W. (2025). A CNN-PINN-DRL driven method for airfoil shape optimization. Engineering *Applications of Computational Fluid Mechanics*, 19(1), Article 2445144. https:// doi. org/ 10.1080/19942060.2024.2445144.

[6] Omenai, S. A. (2024). CFD simulation of steady, compressible flow around NACA 2412 airfoil. *International Journal of Computing and Engineering*, 6(7), 12–26. https://ideas.repec.org/a/bhx/ojijce/v6y2024i7p12-26.

[7] Tejeda-del-Cueto, M. E., Flores-Alfaro, M. A., Toledo-Velázquez, M., & Santos-Cortes, L. D. C. (2023). Airfoil lift coefficient optimization using genetic algorithm and IGP parameterization. *Aerospace*, 11(1), 44. https:// doi. org/ 10. 3390/aerospace11010044.

[8] Wu, M., Yuan, X., Chen, Z., & Wu, Y. H. (2023). Airfoil shape optimization using genetic algorithm coupled deep neural networks. *Physics of Fluids*, 35(8), Article 085140. https://pubs.aip.org/aip/pof/article/35/8/085140/2908296.

[9] Isakhani, H., Xiong, C., Yue, S., & Chen, W. (2020). A bioinspired airfoil optimization technique using Nash genetic algorithm. In *2020 17th International Conference on Ubiquitous Robots (UR)* (pp. 1–6). IEEE. https:// doi. org/ 10.1109/UR49135.2020.9144868.

[10] Google Scholar. (2026). Engineering Applications of Computational Fluid Mechanics [Search database]. https://scholar.google.com/scholar?hl=en&as_sdt=0%2C5&q=Engineering+Applications+of+Computational+Fluid+Mechanics%2C+.

[11] Sadeghimalekabadi, M., Davari, A. R., & Fadaei, M. (2025). Optimization of serrated airfoil for aerodynamics and aeroacoustics via neural network-augmented genetic algorithm. *Proceedings of the Institution of Mechanical Engineers, Part G: Journal of Aerospace Engineering*, 239(14), 1967–1984. https://doi.org/10.1177/ 09544 100251348496.